

## Higherorder FrenkelKontorova modelling of crowdions

S. P. Fitzgerald and D. NguyenManh

Citation: *AIP Conf. Proc.* **999**, 93 (2008); doi: 10.1063/1.2918120

View online: <http://dx.doi.org/10.1063/1.2918120>

View Table of Contents: <http://proceedings.aip.org/dbt/dbt.jsp?KEY=APCPCS&Volume=999&Issue=1>

Published by the [American Institute of Physics](#).

---

### Related Articles

Threading-dislocation blocking by stacking faults formed in an undoped GaN layer on a patterned sapphire substrate

*Appl. Phys. Lett.* **99**, 211901 (2011)

Occupation statistics of the VGa – ON dislocations within n-type gallium nitride

*J. Appl. Phys.* **110**, 033509 (2011)

Initial misfit dislocations in a graded heteroepitaxial layer

*J. Appl. Phys.* **109**, 023510 (2011)

The effect of dopant at the Zr site on the proton conduction pathways of SrZrO<sub>3</sub>: An orthorhombic perovskite

*J. Chem. Phys.* **133**, 064701 (2010)

Individual charge-trapping dislocations in an ionic insulator

*Appl. Phys. Lett.* **95**, 184101 (2009)

---

### Additional information on AIP Conf. Proc.

Journal Homepage: <http://proceedings.aip.org/>

Journal Information: [http://proceedings.aip.org/about/about\\_the\\_proceedings](http://proceedings.aip.org/about/about_the_proceedings)

Top downloads: [http://proceedings.aip.org/dbt/most\\_downloaded.jsp?KEY=APCPCS](http://proceedings.aip.org/dbt/most_downloaded.jsp?KEY=APCPCS)

Information for Authors: [http://proceedings.aip.org/authors/information\\_for\\_authors](http://proceedings.aip.org/authors/information_for_authors)

### ADVERTISEMENT



AIP Advances

*Submit Now*

Explore AIP's new  
open-access journal

- Article-level metrics now available
- Join the conversation! Rate & comment on articles

# Higher-order Frenkel-Kontorova modelling of crowdions

S. P. Fitzgerald and D. Nguyen-Manh

*EURATOM/UKAEA Fusion Association  
Culham Science Centre, Abingdon,  
Oxfordshire, UK, OX14 3DB*

**Abstract.** In this paper we model  $\langle 111 \rangle$  self-interstitial defects, or crowdions, using an extended version of the analytical Frenkel-Kontorova model. We use a more general potential than the traditional sinusoidal one, and find that it can better describe the lattice potentials experienced by crowdions in the body-centred-cubic transition metals, as calculated in density functional theory. We obtain analytical formulae for the crowdion displacement field and elastic strain energy, as functions of three parameters appearing in the Lagrangian, for the generalized lattice potential. Furthermore, we investigate how the more complex structure of the generalized potential affects the *effective* potential experienced by the defect centre-of-mass, using a collective coordinate approach.

**Keywords:** Crowdions, Frenkel-Kontorova model

**PACS:** 61.72Bb, 61.72jj

## INTRODUCTION

The Frenkel-Kontorova model [1] has long been used to describe kinked dislocations in crystalline materials. More recently, it has been used to model crowdions in body-centred-cubic (BCC) metals [2, 3], and clusters of such defects. Crowdions are the most stable defect in the non-magnetic BCC transition metals [4], and although in Fe they are not, highly mobile clusters of self-interstitial atoms (or equivalently prismatic edge dislocation loops) adopt this configuration. The  $\langle 111 \rangle$  string containing the additional atom is modelled as an elastic string interacting with a periodic substrate, which corresponds to the surrounding “perfect” lattice. In most cases, this periodic substrate potential is taken to be  $V_0 \sin^2(\pi x/a)$ , where  $a$  is the lattice spacing in the close-packed direction, since it is the simplest and most analytically tractable option, giving a field of atomic displacements in good agreement with numerical methods. However, recent density functional (DFT) calculations [3] show that the potential acting on a  $\langle 111 \rangle$  string is not well-described by a simple sinusoidal model, particularly for the BCC transition metals in Group 6B of the periodic table. Fig.1, inset shows the DFT-calculated potentials for Mo and Cr, as examples of Group 6B. As far as the model is concerned, all that is required of the potential is periodicity, so the choice of  $V_0 \sin^2(\pi x/a)$  can be viewed as the leading term in a Fourier expansion of a more general potential. Adding a higher-order term,  $V_0 \lambda \sin^2(2\pi x/a)$  (Fig.1, main), allows for a much better fit to the DFT results for the substrate potentials for all the BCC transition metals, at the expense of introducing one additional parameter [3].

Minimizing the resulting energy functional leads to an equation which may still be handled analytically, allowing us to explore a more general soliton solution for the

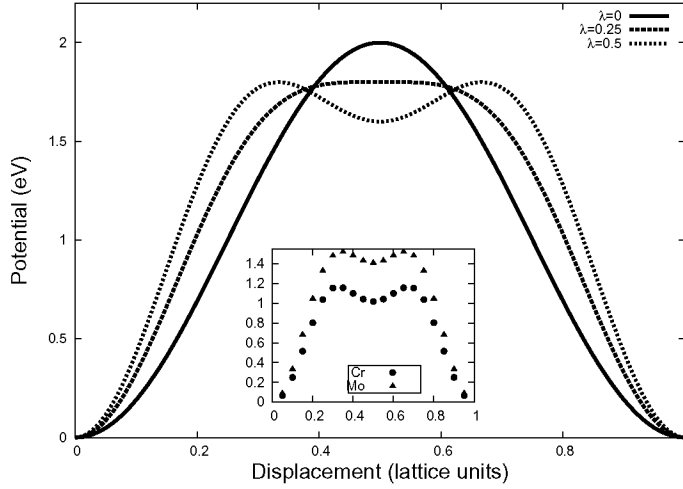


**FIGURE 1.** Substrate potentials for various values of  $\lambda$ . The additional flexibility afforded by  $\lambda$  allows the profile to be adjusted as well as the overall normalization. Inset: DFT potential calculations for Cr and Mo. The higher-order model potential can be fitted accurately to the DFT results for all the BCC transition metals.

crowdion displacement field. Furthermore, the characteristic double-well structure of the Group 6B metals' potentials is shown to persist to the effective potential experienced by the crowdion's centre of mass.

## DISPLACEMENT FIELD SOLUTION

We start from the FK Lagrangian. Writing  $u_n = z_n - na$ , and replacing the discrete displacements by a smoothly-varying function  $u_n(t) \rightarrow u(z, t)$ :

$$\begin{aligned} \mathcal{L} &= \sum_{n=-\infty}^{\infty} \left\{ \frac{m\dot{z}_n^2}{2} - \frac{\beta}{2} (z_{n+1} - z_n - a)^2 - V(z_n) \right\} \\ &\rightarrow \int_{-\infty}^{\infty} \frac{dz}{a} \left\{ \frac{m}{2} \left( \frac{\partial u}{\partial t} \right)^2 - \frac{\beta a^2}{2} \left( \frac{\partial u}{\partial z} \right)^2 - V(u) \right\}. \end{aligned} \quad (1)$$

With

$$V(u) = V_0 \left( \sin^2 \frac{\pi u}{a} + \lambda \sin^2 \frac{2\pi u}{a} \right) \quad (2)$$

for the potential, the Euler-Lagrange equation reads

$$m \frac{\partial^2 u}{\partial t^2} - \beta a^2 \frac{\partial^2 u}{\partial z^2} = -\frac{V_0 \pi}{a} \left[ \sin \frac{2\pi u}{a} + 2\lambda \sin \frac{4\pi u}{a} \right]. \quad (3)$$

For the static case  $\dot{u} = 0$  this becomes

$$w'' = \mu^2 (\sin w + 2\lambda \sin 2w), \quad (4)$$

where  $w = 2\pi u/a$  and  $\mu^2 = 2\pi^2 V_0/\beta a^4$ . This is valid provided the displacements vary slowly with  $z$ . The limit  $\lambda \rightarrow 0$  returns the conventional FK model. With standard “kink” boundary conditions at infinity ( $u(-\infty) = a, u(\infty) = 0$ ), corresponding to one extra atom in the string, this leads to

$$\begin{aligned} \frac{1}{2} \left( \frac{dw}{dz} \right)^2 &= \mu^2 (1 - \cos w + \lambda (1 - \cos 2w)) \\ &= 2\mu^2 \left( \sin^2 \frac{w}{2} + \lambda \sin^2 w \right), \end{aligned} \quad (5)$$

and hence

$$\frac{dw}{dz} = \pm 2\mu \sqrt{\sin^2 \frac{w}{2} + \lambda \sin^2 w}, \quad (6)$$

where we take the negative square root as we define the scaled displacement  $w$  to be  $2\pi$  at  $-\infty$ , decreasing to 0 at  $\infty$ . This can be integrated to give

$$z - z_0 = \frac{1}{\mu\alpha} \operatorname{arcsinh} \left[ \frac{\alpha}{\tan \frac{w}{2}} \right], \quad (7)$$

where  $\alpha^2 = 1 + 4\lambda$ , and  $z_0$  is an arbitrary constant representing the centre-of-mass of the crowdion. The physics contained in the sine-Gordon-like Eq.(4) is independent of  $z_0$ , reflecting the continuum limit we have taken. Physically, this corresponds to the period of the substrate potential going to zero, and in this approximation the crowdion can move freely through the lattice. The only information about the substrate potential is that retained in the shape of the kink solution. Inverting and returning to the original variables we arrive at

$$u(z) = \frac{a}{\pi} \arctan \left[ \frac{\alpha}{\sinh(\mu\alpha(z - z_0))} \right] \quad (8)$$

for the displacement field. This solution was previously derived for kinks in dislocation lines [5, 6]. Note the difference with respect to the Gudermannian solution of the conventional FK model ( $\lambda = 0 \rightarrow \alpha = 1$ ):

$$u_0(z) = \frac{2a}{\pi} \arctan [\exp [-\mu(z - z_0)]] . \quad (9)$$

The argument of the inverse tangent in this case is always positive, so an additional factor of two is required to cover the range of displacement  $(a, 0)$ , which leads to a slight subtlety as regards the function (8) (and the associated boundary conditions): it is discontinuous at the origin. To remedy this, we may add  $a$  to the negative- $z$  part of the solution, *i.e.*  $u \rightarrow u + a\Theta(-z)$ , with  $\Theta$  the Heaviside function. This is entirely consistent with (5), and the boundary conditions are now satisfied.

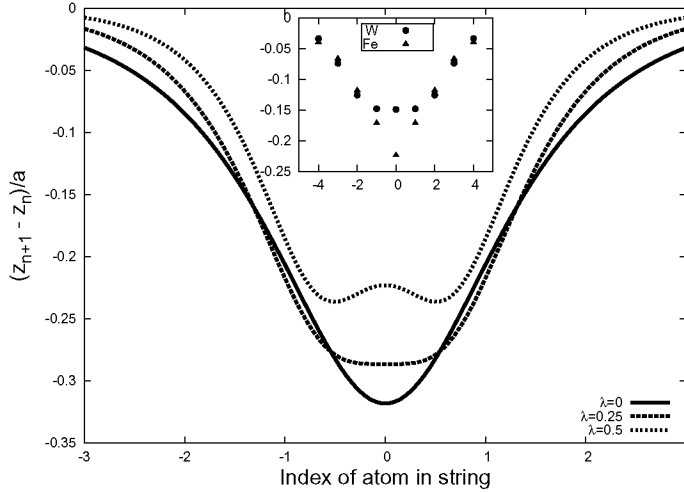


**FIGURE 2.** Displacement gradients for various values of  $\lambda$ . The displacement field arising from the more general potential can better accommodate the DFT-calculated results (Inset: DFT displacement gradients for W and Fe).

Fig.2, inset shows the DFT-calculated displacement gradients for W and Fe. The main part of the figure illustrates the enhanced versatility of the analytic solution arising from the more general potential. The solution can be accurately fitted to the DFT results all the BCC transition metals [3].

## CROWDION ENERGIES

The total energy is given by

$$E = \int_{-\infty}^{\infty} \mathcal{E} \frac{dz}{a}, \quad (10)$$

where

$$\mathcal{E} = \frac{\beta a^2}{2} \left( \frac{du}{dz} \right)^2 + V_0 \left( \sin^2 \frac{\pi u}{a} + \lambda \sin^2 \frac{2\pi u}{a} \right). \quad (11)$$

Substituting Eq.(8) (the addition of  $a$  to the negative- $z$  part of the solution is irrelevant here, since  $\mathcal{E}$  depends on  $u$  only via derivatives and  $a$ -periodic functions), and using  $4\lambda = \alpha^2 - 1$ , we arrive at

$$\mathcal{E} = \frac{\alpha^4 \cosh^2 \mu \alpha z}{(\alpha^2 + \sinh^2 \mu \alpha z)^2} \left[ \frac{\beta a^4 \mu^2}{2\pi^2} + V_0 \right]. \quad (12)$$

The terms in square brackets represent the contributions to the total energy from the tension in the string and the interaction with the substrate potential. In fact, they are equal as can be seen simply from the definition of  $\mu$ . Thus, the soliton solution partitions the

energy equally between the two contributions, as with the conventional FK sine-Gordon soliton. The limit  $\lambda \rightarrow 0$  corresponds to  $\alpha \rightarrow 1$ , and the integrand in the above reduces to  $\text{sech}^2(\mu z)$ . This recovers the energy expression for the sine-Gordon solution. For  $\alpha > 1$ , the integral may still be performed analytically, and yields the final result

$$E = \frac{a}{\pi} \sqrt{2V_0\beta} \left( \alpha + \frac{\cosh^{-1} \alpha}{\sqrt{\alpha^2 - 1}} \right) \rightarrow \frac{2a}{\pi} \sqrt{2V_0\beta} \text{ as } \alpha \rightarrow 1. \quad (13)$$

## POTENTIAL FOR THE DEFECT CENTRE-OF-MASS

In the continuum limit, the energy is independent of the crowdion's centre-of-mass, *i.e.* it is translation-invariant (similar to a Goldstone mode in field theory). To return to the discrete description, we follow [7] and start by writing the total energy as

$$\begin{aligned} E &= \sum_{n=-\infty}^{\infty} \left( \frac{\beta}{2} (z_{n+1} - z_n - a)^2 + V(u_n) \right) \\ &\rightarrow 2 \sum_{n=-\infty}^{\infty} V(u_n). \end{aligned} \quad (14)$$

This is permissible since the soliton solution partitions the energy equally between the interactions between atoms in the crowdion string, and those between the string atoms and the surrounding strings, encoded in the substrate potential. For the  $u_n$  we use the continuum solution for the displacement field Eq.(8), evaluated at the discrete lattice sites  $z = na$ :

$$u_n = u(na) = \frac{a}{\pi} \arctan \left[ \frac{\alpha}{\sinh(\mu\alpha(na - x_0))} \right]. \quad (15)$$

A perturbative series for the energy as a function of  $x_0$  can be obtained via the Poisson summation formula:

$$\begin{aligned} E(x_0) &= 2V_0\alpha^4 \sum_{n=-\infty}^{\infty} \frac{\cosh^2(\alpha\mu(na - x_0))}{(\alpha^2 + \sinh^2(\alpha\mu(na - x_0)))^2} \\ &= 2V_0\alpha^4 \sum_{m=-\infty}^{\infty} \int_{-\infty}^{\infty} e^{2\pi imk} \frac{\cosh^2(\alpha\mu(ka - x_0))}{(\alpha^2 + \sinh^2(\alpha\mu(ka - x_0)))^2} dk \\ &= 2V_0\alpha^4 \left\{ \int_{-\infty}^{\infty} \frac{\cosh^2(\alpha\mu(ka - x_0))}{(\alpha^2 + \sinh^2(\alpha\mu(ka - x_0)))^2} dk \right. \\ &\quad \left. + 2 \sum_{m=1}^{\infty} \int_{-\infty}^{\infty} \cos(2\pi mk) \frac{\cosh^2(\alpha\mu(ka - x_0))}{(\alpha^2 + \sinh^2(\alpha\mu(ka - x_0)))^2} dk \right\} \\ &\equiv E_0 + 2 \sum_{m=1}^{\infty} I_m(x_0), \end{aligned} \quad (16)$$

where  $E_0$  is the energy of the crowdion when discreteness effects are neglected, and the sum represents a Fourier expansion of the potential the centre-of-mass is subject

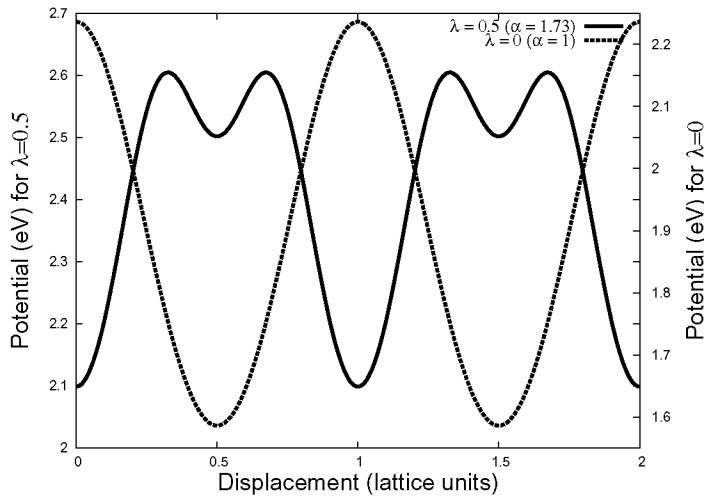


**FIGURE 3.** Total energy of the crowdion as a function of its centre-of mass, for  $\lambda = 0, 0.5$ , including the first three terms in the discrete Fourier expansion. Different scales are used as the constant “continuum energy”  $E_0$  shifts the baseline of the potential experienced by the crowdion’s centre-of-mass.  $\mu = 2.1$  in these examples.

to, due to the discreteness (the  $I_m$  are given in the Appendix.) This potential is distinct from the lattice substrate potential  $V$ : the above procedure integrates out the degrees of freedom corresponding to the positions of the individual atoms, and the position of the centre-of-mass becomes a collective coordinate. The effect of the more general potential is striking, and is illustrated in Fig.(3). In the  $\lambda = 0$  case, the second and third terms in the series are negligible, and the centre-of-mass potential is almost purely sinusoidal ( $\mu = 2.1$  in both cases). When  $\lambda = 0.5$ , a deep local minimum appears. This is due to the increased importance of the higher order terms in the Fourier series Eq.(16). Note also the shift in the major minima by half a period: this is because the atom closest to the crowdion’s centre may now sit in the local minimum, (of the original lattice potential), as opposed to atop a local maximum in the sinusoidal case. This central atom is the one most displaced from its equilibrium position with respect to the perfect lattice, and so makes the largest contribution to the defect’s energy. The relative depths of the wells are still small however, reflecting the ease with which the crowdion can migrate through the lattice (different scales are used to better compare the potential landscapes in which the defect migrates; the absolute energy level is shifted by the relative variation of the  $E_0$  continuum term).

## CONCLUSIONS

In this paper we have used the Frenkel-Kontorova model, with a modified functional form for the potential, to model  $\langle 111 \rangle$  crowdion defects in BCC crystals. This generalization allows more realistic modelling of such defects in the BCC transition metals, since

the conventional sinusoidal form does not well describe recent DFT calculations of the substrate potential, especially for metals in Group 6B of the periodic table [3]. The model remains analytically tractable, and expressions for the field of atomic displacements and the elastic strain energy were derived in the continuum approximation. Furthermore, the effects of lattice discreteness were considered by a collective-coordinate approach, and the double-well structure of the general potential can persist to the effective potential experienced by the crowdion's centre-of-mass. Direct experimental observation of single self-interstitial atom defects is difficult or impossible, because of their size. However, information about the migration behaviour of these defects can be obtained indirectly, for example through resistivity recovery experiments [8], which report a large difference in the migration temperatures between metals in Group 5B and those in Group 6B. The more complex potential landscape in which the crowdion moves will affect its mobility, and this may help to explain the large difference between Group 5B (where the substrate potential is close to the sinusoidal form) and Group 6B (which exhibits more pronounced local minima).

## ACKNOWLEDGMENTS

The authors would like to thank S. Dudarev and A. Thyagaraja for stimulating discussions. This work is supported by the UK Engineering and Physical Sciences Research Council and the European Community under the contract of Association between EURATOM and UKAEA. The views and opinions expressed herein do not necessarily reflect those of the European Commission.

## REFERENCES

1. O. M. Braun, and Y. S. Kivshar, *Phys. Rep.* **306**, 1–108 (1998).
2. D. I. Pushkarov, *Sov. JETP* **37**, 322 – 325 (1973).
3. D. Nguyen-Manh, and S. P. Fitzgerald, *Submitted to Phil. Mag. Lett.* (2007).
4. D. Nguyen-Manh, A. P. Horsfield, and S. L. Dudarev, *Phys. Rev. B* **73**, 020101R (2006).
5. F. Frank, and J. van der Merwe, *Proc. Roy. Soc. Lon.* **A 200**, 125–134 (1949).
6. A. Seeger, and P. Schiller, “Kinks in dislocation lines,” in *Physical Acoustics: Principles and Methods (Volume 3, Part A, p361)*, edited by W. P. Mason, Academic Press Inc, 1966, ISBN 0124779085.
7. A. M. Kosevich, *The Crystal Lattice*, Wiley-VCH, 1999, ISBN 3527402209.
8. P. Ehrhart, P. Jung, H. Shultz, and H. Ullmaier, “,” in *Atomic Defects in Metals*, edited by H. Ullmaier, Springer-Verlag, 1991.

## APPENDIX: EVALUATION OF FOURIER COEFFICIENTS $I_m$

The coefficients  $I_m$  are defined by

$$I_m = \int_{-\infty}^{\infty} \cos(2\pi mk) \frac{\cosh^2(\alpha\mu(ka - x_0))}{(\alpha^2 + \sinh^2(\alpha\mu(ka - x_0)))^2} dk, \quad (17)$$

which does not appear in the standard tables, so we give its evaluation for completeness. If we define

$$\begin{aligned} p &= \alpha\mu(ak - x_0); \\ 2\pi mk &= \frac{2\pi m(p + \alpha\mu x_0)}{\alpha\mu a} \equiv \xi p + \eta, \text{ then} \end{aligned} \quad (18)$$

$$I_m = \frac{1}{\alpha\mu a} \int_{-\infty}^{\infty} \frac{(\cos \xi p \cos \eta - \sin \xi p \sin \eta) \cosh^2 p}{(\alpha^2 + \sinh^2 p)^2} dp. \quad (19)$$

and we can instead consider the integral

$$\begin{aligned} \mathcal{I} &= \int_{-\infty}^{\infty} \frac{e^{i\xi p} \cosh^2 p}{(\alpha^2 + \sinh^2 p)^2} dp. \text{ Then} \\ I_m &= \frac{1}{\alpha\mu a} \{ \cos \eta \operatorname{Re} [\mathcal{I}] - \sin \eta \operatorname{Im} [\mathcal{I}] \}. \end{aligned} \quad (20)$$

Now

$$\begin{aligned} \mathcal{I} &= -\frac{\partial \mathcal{J}}{\partial \alpha^2}; \quad \mathcal{J} = \int_{-\infty}^{\infty} \frac{e^{i\xi p} \cosh^2 p}{\alpha^2 + \sinh^2 p} dp. \\ &= \int_{-\infty}^{\infty} e^{i\xi p} \left\{ 1 + \frac{1 - \alpha^2}{\alpha^2 + \sinh^2 p} \right\} dp. \end{aligned} \quad (21)$$

The first term in the braces will go to a  $\delta$ -function, but since it does not depend on  $\alpha^2$  we may ignore it, and write

$$\begin{aligned} \mathcal{I} &= -\frac{\partial \bar{\mathcal{J}}}{\partial \alpha^2}; \quad \bar{\mathcal{J}} = (1 - \alpha^2) \int_{-\infty}^{\infty} \frac{e^{i\xi p}}{\alpha^2 + \sinh^2 p} dp, \\ \frac{\bar{\mathcal{J}}}{(1 - \alpha^2)} &= \int_0^{\infty} \frac{2q^{i\xi/2} dq}{q^2 + (4\alpha^2 - 2)q + 1} \end{aligned} \quad (22)$$

p

where  $q = e^{2p}$ , which is amenable to contour integration. Finally

$$\bar{\mathcal{J}} = \frac{4\pi i(1 - \alpha^2)}{(1 - e^{-\xi\pi})(q_1 - q_2)} \left( q_1^{i\xi/2} - q_2^{i\xi/2} \right). \quad (23)$$

where

$$q_{1,2} = 1 - 2\alpha^2 \pm 2\alpha\sqrt{\alpha^2 - 1}. \quad (24)$$

Substituting the values of  $q_{1,2}$ , and operating with  $-\partial/\partial\alpha^2$  leads eventually to

$$\begin{aligned} I_m &= \frac{1}{\alpha\mu a} \frac{\pi}{2\alpha^2} \cos \eta \operatorname{cosech} \left( \frac{\xi\pi}{2} \right) \times \\ &\left\{ \xi \cos \left( \frac{\xi}{4} \ln \frac{q_1}{q_2} \right) - \frac{1}{\alpha\sqrt{\alpha^2 - 1}} \sin \left( \frac{\xi}{4} \ln \frac{q_1}{q_2} \right) \right\}, \end{aligned} \quad (25)$$

which agrees exactly with numerical evaluation of Eq.(17) across the relevant range of parameters. In the limit  $\lambda \rightarrow 0$ ,  $\alpha \rightarrow 1$

$$I_1 \rightarrow \frac{\pi^2}{\mu^2 a^2} \operatorname{cosech} \left( \frac{2\pi}{\mu a} \right) \cos \left( \frac{2\pi x_0}{a} \right), \quad (26)$$

which may be compared with the results in Chapter 9.4 of Ref. [7].